



J. Serb. Chem. Soc. 79 (8) 993–1005 (2014)
JSCS–4642

Effect of the orientation of the initially formed grains on the final morphology of electrodeposited lead*

NEBOJŠA D. NIKOLIĆ^{1#}, KONSTANTIN I. POPOV^{1,2*}, EVICA R. IVANOVIĆ³
and GORAN BRANKOVIĆ^{4#}

¹ICTM – Institute of Electrochemistry, University of Belgrade, Njegoševa 12, P. O. Box 473, 11001 Belgrade, ²Faculty of Technology and Metallurgy, University of Belgrade, Karnegijeva 4, P. O. Box 3503, 11001 Belgrade, ³Faculty of Agriculture, University of Belgrade, Nemanjina 6, Belgrade-Zemun and ⁴Institute for Multidisciplinary Research, University of Belgrade, Kneza Višeslava 1a, Belgrade, Serbia

(Received 11 December 2013, revised 20 January, accepted 21 January 2014)

Abstract: The processes of Pb electrodeposition under diffusion control were examined by scanning electron microscopy (SEM) of the formed crystals. The orientation of grains of hexagonal shape formed in the initial stage of electrodeposition strongly affected the final morphology of the Pb crystals. The formation of Pb crystals of the different shape from the same initial shape was discussed in terms of the effect of orientation of initially formed grains on the type of diffusion control. A spherical diffusion layer was formed around the tip of the hexagonal-shaped grain oriented with its tip towards the bulk solution that led to the formation of elongated crystals in the growth process. On the other hand, a cylindrical type of diffusion was responsible for the growth of hexagonal-shaped grains oriented with the lateral side towards the bulk solution. Pb crystals with well-defined sides parallel to the surface area of the macroelectrode were formed under this type of diffusion.

Keywords: electrodeposition; lead; crystal; spherical diffusion; cylindrical diffusion; scanning electron microscope (SEM).

INTRODUCTION

Thanks to its specific characteristics, such as extremely high reactivity and superconductivity, lead has found an application in many very important technologies.¹ Some of these technologies are related with a production of high purity active material for acid batteries,² for semiconductors,^{3,4} and in the fabrication of electrochromic devices.⁵ Electrodeposition technique is very attractive way to

• In memory of Prof. Dr. John O'M. Bockris.

* Corresponding author. E-mail: kosta@tmf.bg.ac.rs

Serbian Chemical Society member.

doi: 10.2298/JSC131211006N

obtain Pb in the form suitable for application in various technologies. The morphology of electrodeposited Pb, the growth rate, particle size and number density can be easily regulated by the choice and control of parameters such as deposition potential or current density, regime of electrolysis, time, temperature and solution composition.

Lead belongs to the group of normal metals that are characterized by high exchange current density values, low melting points and high overpotentials for hydrogen discharge.^{6,7} Regardless of the type of electrolyte, electrodeposition of lead occurs under mixed ohmic–diffusion or even full ohmic control of the electrodeposition.^{8–11} The ratio of the ohmic to the overall control of the electrodeposition increases with increasing concentration of Pb^{2+} so that the electrodeposition process becomes a full ohmic controlled one at high concentrations of Pb^{2+} .^{8,11}

Regular crystals were the main morphological forms obtained in electrodepositions at overpotentials in the ohmic control region.^{11,12} The shape of these crystals did not depend on the type of electrolyte. On the contrary, the shape of the dendrites formed under the diffusion control was strongly influenced by the type of electrolyte used. Considering the Wranglen definition of a dendrite,¹³ dendrites of the secondary (S) type, constructed from a stalk and primary and secondary branches, were electrodeposited from complex electrolytes, such as acetate⁹ and alkaline¹⁰ electrolytes. Needle-like and dendrites constructed from stalk and only primary branches (the primary (P) type) were formed during electrodepositions from basic (nitrate) electrolytes. In addition to dendrites, irregular crystals of various shapes were also formed during electrodepositions under diffusion control. The aim of this study was to investigate the mechanism of the formation of these irregular Pb crystals.

EXPERIMENTAL

Electrodeposition of lead was performed in an open cell from 0.40 M $\text{Pb}(\text{NO}_3)_2$ in 2.0 M NaNO_3 at room temperature (22.0 ± 0.5 °C). Lead was electrodeposited at overpotentials of 50 and 75 mV, with amounts of the electricity of 0.10 and 0.95 mA h cm^{-2} . Doubly distilled water and analytical grade chemicals were used for the preparation of the solution for electrodeposition of lead. All electrodepositions were performed on vertical cylindrical copper electrodes. The geometric surface areas of the copper electrodes were 0.25 cm^2 for the SEM analyses of the obtained Pb deposits and 0.50 cm^2 for recording the polarization curve. The polarization curve for the electrodeposition of lead was recorded potentiostatically by changing the overpotential in 5 mV steps. In order to obtain a reproducible shape of the polarization curve for this reaction, the following experimental procedure,^{8,14} usual for the recording of the polarization curves of fast electrodeposition processes, was applied. At low overpotentials up to 55 mV (Fig. 1), the values of the current obtained after reaching steady-state values were used for constructing the polarization curves. Since at the overpotentials after the inflection point (55 mV) on the polarization curve in Fig. 1, the current increased dramatically over

time, the values were recorded immediately after setting the selected overpotential values were used.

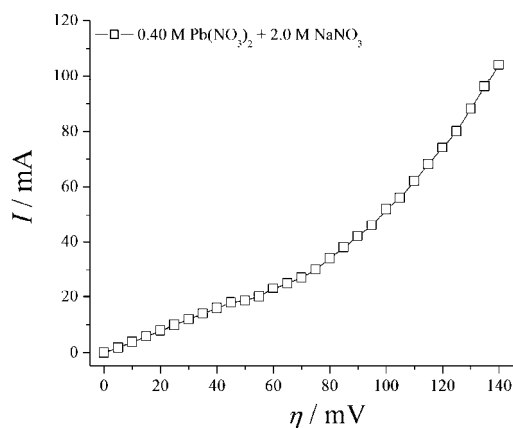


Fig. 1. The polarization curve for lead electrodeposition from 0.40 M $\text{Pb}(\text{NO}_3)_2$ in 2.0 M NaNO_3 . The surface area of working electrode was 0.50 cm^2 .

The reference and counter electrodes were of pure lead. The counter electrode was lead foil with surface area of 0.80 dm^2 and was placed close to the cell walls. The reference electrode was lead wire, the tips of which were positioned at a distance of about 0.2 cm from the surface of the working electrode. The working electrodes were placed in the centre of the cell, at the same location for each experiment.

A Tescan digital scanning electron microscope was used for the examination of the morphology of the Pb deposits.

RESULTS AND DISCUSSION

Polarization curve for Pb electrodeposition from 0.40 M $\text{Pb}(\text{NO}_3)_2$ in 2.0 M NaNO_3 is shown in Fig. 1. The interval of overpotentials between 0 and 45 mV corresponds to ohmic control. The diffusion control commences at an overpotential of 45 mV and the inflection point is observed at 55 mV.

SEM images of the Pb deposits formed during the initial stages of electrodeposition at overpotentials of 50 and 75 mV are shown in Fig. 2a and b, and Fig. 2c and d, respectively. It is necessary to note that both overpotentials corresponded to electrodeposition under diffusion control. At both overpotentials, hexagonal-shaped grains were formed together with numerous other grains of various shapes that showed well-defined crystal planes. Although the shape of the hexagonal grains was the same in both cases, the orientations of these grains were completely different. In the Pb deposit electrodeposited at 50 mV, the hexagonal-shaped grain was oriented with its lateral side towards the bulk solution (Fig. 2a and b). On the other hand, the hexagonal-shaped grain in the Pb deposit electrodeposited at 75 mV was oriented with its tip towards the bulk solution (Fig. 2c and d).

Analysis of Fig. 2 clearly confirms that nucleation did not occur simultaneously over the entire cathode surface, but it was a process extended in time so that

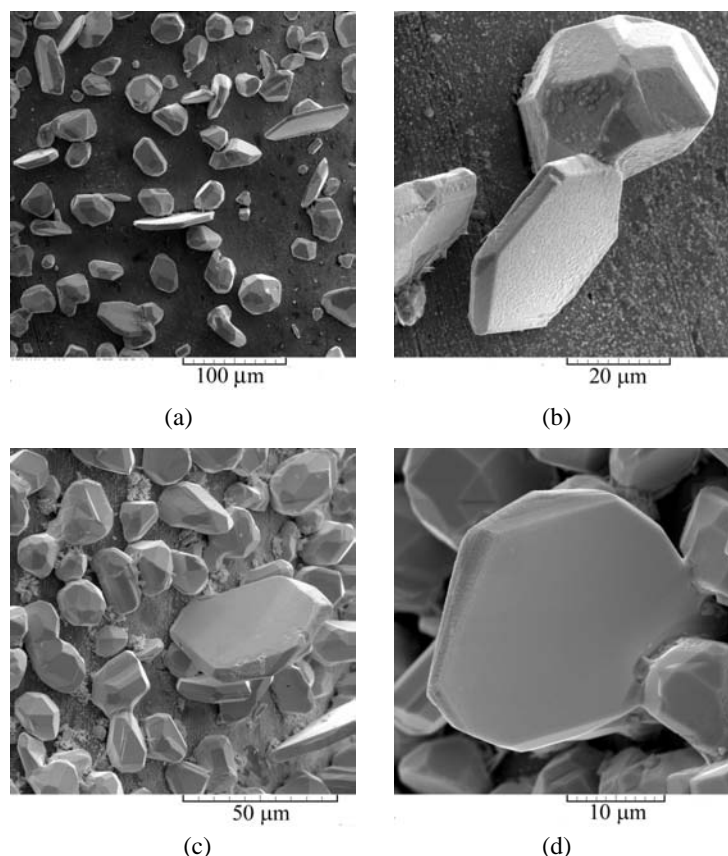


Fig. 2. SEM images of the Pb deposits formed in the initial stages of Pb electrodeposition from 0.40 M $\text{Pb}(\text{NO}_3)_2$ in 2.0 M NaNO_3 at overpotentials of: a) and b) 50 mV, and c) and d) 75 mV. The amount of electricity was $0.10 \text{ mA h cm}^{-2}$.

grains generated earlier may be considerably larger in size than those generated later.¹⁵ In the case of fast electrochemical processes, nucleation exclusion zones around already existing nuclei are formed,^{16,17} as seen from Fig. 2. This process causes a periodicity in the structure of polycrystalline deposit.^{18–20} With increasing the electrodeposition time, due to the current density distribution effect,²¹ further nucleation and growth primarily occurs at these hexagonal-shaped grains. The final forms of the Pb crystals obtained at overpotentials of 50 and 75 mV with an amount of electricity of $0.95 \text{ mA h cm}^{-2}$ are shown in Fig. 3. From Fig. 3, it can be seen that the Pb crystals formed at an overpotential of 50 mV (Fig. 3a and b) were completely different in shape to those formed at 75 mV (Fig. 3c and 3d). The characteristics of the 2D (two-dimensional) Pb crystals formed at 50 mV were well-developed sides parallel to the surface area of the macroelectrode (crystals denoted with A, B, C and D in Fig. 3a and the crystal shown in Fig. 3b).

The 2D crystals obtained at 75 mV were with sharp tips as can be seen from Fig. 3c and d.

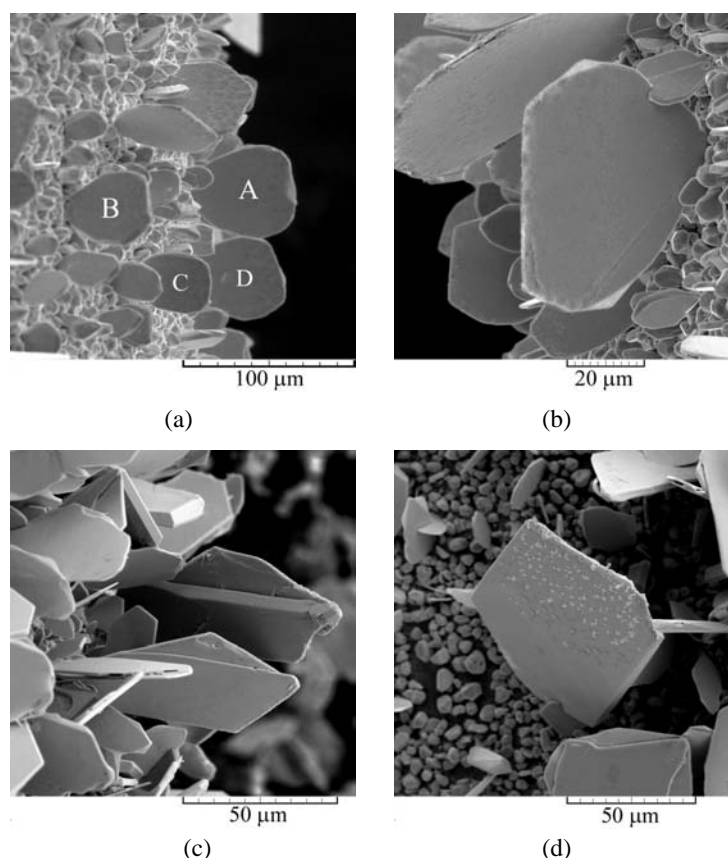


Fig. 3. SEM images showing the shape of crystals formed by electrodeposition processes from 0.40 M $\text{Pb}(\text{NO}_3)_2$ in 2.0 M NaNO_3 with amount of electricity of $0.95 \text{ mA h cm}^{-2}$. The overpotentials of electrodeposition were: a) and b) 50 mV, and c) and d) 75 mV.

Hence, the same shape of Pb grains formed in the initial stage of the electrodeposition (Fig. 2) gave completely different final shapes of the Pb crystals (Fig. 3). Considering that the electrodeposition processes at both overpotentials were under diffusion control, it is very clear that the orientation of the grains formed in the initial stages of electrodeposition played an important, or even crucial, role in the mechanism of the formation of the final forms of the Pb crystals. A schematic presentation of the processes of formation and growth of the crystals in dependence of the orientation of the initially formed grains is given in Fig. 4.

The equation of the cathodic polarization curve for a flat or a large spherical electrode of a massive metal is given by Eq. (1):¹⁵

$$j = \frac{j_0(f_c - f_a)}{1 + \frac{j_0 f_c}{j_L}} \quad (1)$$

where j , j_0 and j_L are the current density, the exchange current density and the limiting diffusion current density, respectively, and:

$$f_c = 10^{\frac{\eta}{b_c}} \quad (2)$$

$$f_a = 10^{-\frac{\eta}{b_a}} \quad (3)$$

where b_c and b_a are the cathodic and anodic Tafel slopes and η is the overpotential. Equation (1) is modified for use in electrodeposition of metals by taking cathodic current density and overpotential as positive.

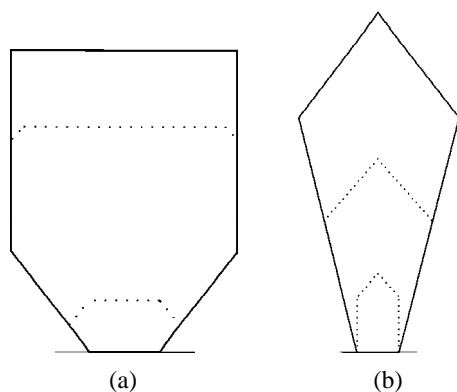


Fig. 4. Time dependent simulation of growth of the differently oriented crystals.

The cathodic limiting diffusion current density for steady-state linear diffusion, j_L , is given by Eq. (4):

$$j_L = \frac{nFDc_0}{\delta} \quad (4)$$

where n is the number of transferred electrons, F is the Faraday constant, D and c_0 are the diffusion coefficient and bulk concentration of the depositing ion, respectively, and δ is the thickness of the diffusion layer of the macroelectrode.

The parallel sides of initially and finally formed Pb crystals (Fig. 3a and b) clearly indicate that the growth of the hexagonal-shaped grains (Fig. 2a and b) can be ascribed to a cylindrical type of diffusion around their top edges. A schematic presentation of a crystal that obeys this type of diffusion is presented in Fig. 5a. The limiting diffusion current density to the cylindrical electrode, $j_{L,c}$ growing inside the diffusion layer of the macroelectrode is given by Eq. (5):^{22,23}

$$j_{L,c} = \frac{nFDc_0}{r \ln \frac{r+d}{r}} \quad (5)$$

where $d = (\pi Dt)^{0.5}$, r is the radius of the flat dendrite precursor and $r \ll l$. Assuming to a first approximation that under steady state conditions d corresponds to thickness of the diffusion layer of the macroelectrode, δ , then the condition $\delta \gg r$ is valid and Eq. (5) can be rewritten in the form:

$$j_{L,c} = \frac{nFDc_0}{r \ln \frac{\delta}{r}} \quad (6)$$

or in the form:

$$j_{L,c} = \frac{j_L}{\frac{\delta}{r} \ln \frac{\delta}{r}} \quad (7)$$

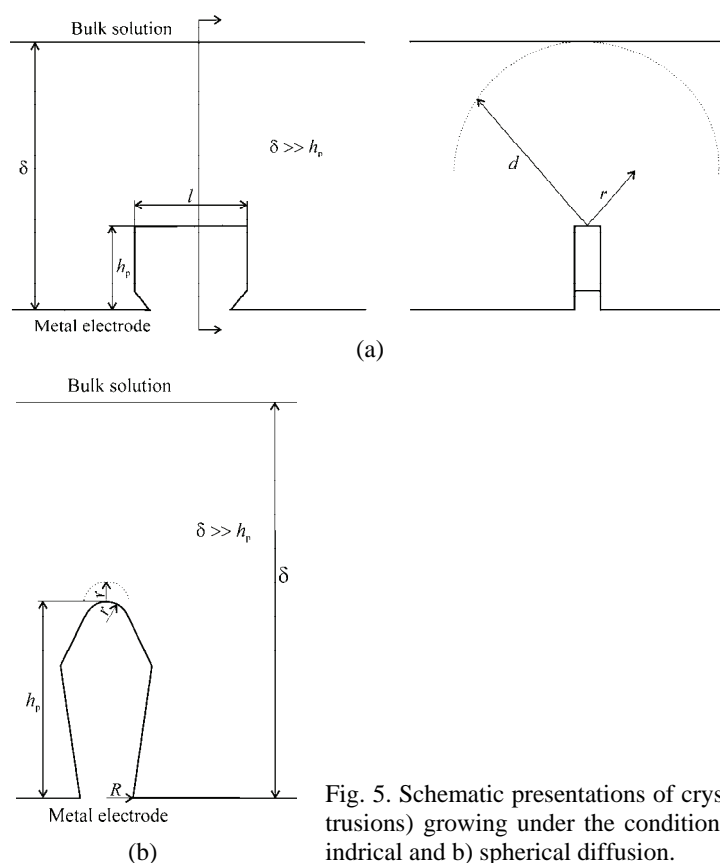


Fig. 5. Schematic presentations of crystals (or protrusions) growing under the conditions of: a) cylindrical and b) spherical diffusion.

In the initial stage of the electrodeposition, the sizes of all grains are similar to each other, and the cylindrical type of diffusion cannot be established due to the overlapping of the diffusion zones. Then, the maximum current density to the surface of grain (top edge) corresponds to the limiting diffusion current density, j_L . Dendritic growth may be expected for:

$$j_L < j_{\text{tip,c}} \quad (8)$$

i.e., when the current density under mixed controlled deposition to the tip of the grain, $j_{\text{tip,c}}$, becomes larger than the linear limiting diffusion current density.

Substitution of $j_{L,c}$ from Eq. (7) into Eq. (1) instead of j_L gives the equation for the tip current density, $j_{\text{tip,c}}$, as:

$$j_{\text{tip,c}} = \frac{j_0(f_c - f_a)}{1 + \frac{j_0 f_c}{j_L} \frac{r}{\delta} \ln \frac{\delta}{r}} \quad (9)$$

Relation (8) can then be written in the form:

$$j_L < \frac{j_0(f_c - f_a)}{1 + \frac{j_0 f_c}{j_L} \frac{r}{\delta} \ln \frac{\delta}{r}} \quad (10)$$

If it is assumed that $r \ll \delta$, which is true for the assumed meaning of r and δ , then:

$$\frac{r}{\delta} \ln \frac{\delta}{r} \ll 1$$

and the overpotential function is larger than the j_L/j_0 ratio. Using Eq. (2), it follows that the minimum overpotential at which the growth of a dendrite is possible, η_i , is given by Eq. (11):

$$\eta_i = b_c \log \frac{j_L}{j_0} \quad (11)$$

Hence, initiation of dendritic growth is possible only at overpotentials larger than η_i .

On the other hand, it could be assumed that the condition of spherical diffusion is fulfilled around the tip of a hexagonal-shaped grain oriented normally to the electrode surface, *i.e.*, with the tip towards the bulk of the solution (Fig. 2c and d). A schematic presentation of a crystal buried deep in the diffusion layer of the macroelectrode around the tip of which a spherical diffusion layer is formed is shown in Fig. 5b. The local limiting diffusion current density is larger at the tips of such crystals than the corresponding linear diffusion current density, and for this reason, the tip of a crystal will grow faster than the other parts of a crystal where the conditions of cylindrical diffusion are fulfilled.^{24,25} As a result of this

process, elongated crystals, like those shown in Fig. 3c and d, are formed. Then, the formation of the elongated crystals could be explained in the following way.

At the tip of a hexagonal-shaped grain, the lateral flux cannot be neglected and the situation can be approximated by assuming a spherical diffusion current density, $j_{L,s}$, given by Eq. (12):^{24,25}

$$j_{L,s} = \frac{nFDc^*}{r} \quad (12)$$

where c^* is the concentration of the diffusing species at a distance r from the tip, assuming that around the tip a spherical diffusion layer having a thickness equal to the radius of the protrusion tip is formed.²⁶

If deposition to the macroelectrode is under full diffusion control, the distribution of the concentration, c , inside the linear diffusion layer is given by Eq. (13):²⁷

$$c = c_0 \frac{h}{\delta} \quad (13)$$

where $0 \leq h \leq \delta$. In the present case, it will be:

$$c^* = c_0 \frac{h_p + r}{\delta} \quad (14)$$

and

$$j_{L,s} = j_L \left(1 + \frac{h_p}{r} \right) \quad (15)$$

because of Eqs. (4), (12) and (14), where h_p is height of a protrusion (*i.e.*, crystal in the present case).

Substitution of $j_{L,s}$ from Eq. (15) into Eq. (1) produces for $h_p/r \gg 1$ after rearranging Eq. (16):

$$j_{tip,s} = j_{0,tip}(f_c - f_a) \quad (16)$$

where $j_{tip,s}$ and $j_{0,tip}$ are the current density and the exchange current density at the tip of the protrusion, respectively. Then, the electrodeposition process to the tip of such protrusion inside the diffusion layer of the macroelectrode is an activation-controlled process relative to the surrounding electrolyte, but it is under mixed control relative to the bulk solution. The maximum growth rate at a given overpotential corresponds to activation-controlled deposition, occurring on the tip of a crystal, where spherical diffusion control can be established.

Naturally, the concentration of depositing ions at the tip of crystal, c_{tip} , is given by Eq. (17):

$$c_{\text{tip}} = c_0 \frac{h_p}{\delta} \quad (17)$$

According to Newman,²⁸ the exchange current density at the tip of a protrusion growing inside the diffusion layer of a macroelectrode, $j_{0,\text{tip}}$, is given by Eq. (18):

$$j_{0,\text{tip}} = j_0 \left(\frac{c_{\text{tip}}}{c_0} \right)^\gamma \quad (18)$$

where:

$$\gamma = \frac{d(\log j_0)}{d(\log c_0)} \quad (19)$$

and j_0 corresponds to the exchange current density for a surface concentration, c_0 , equal to the bulk concentration, or:

$$j_{0,\text{tip}} = j_0 \left(\frac{h_p}{\delta} \right)^\gamma \quad (20)$$

because of Eq. (17). Substitution of $j_{0,\text{tip}}$ from Eq. (20) into Eq. (16) produces:

$$j_{\text{tip},s} = j_0 \left(\frac{h_p}{\delta} \right)^\gamma (f_c - f_a) \quad (21)$$

and the minimum overpotential at which dendritic growth is possible is:

$$\eta_i = b_c \log \frac{j_L}{j_0}$$

for $h_p = \delta$ and $f_c \gg f_a$, if the condition for dendritic growth initiation is $j_L < j_{\text{tip},s}$. Hence, both kinds of dendrites can grow at the same deposition overpotential.

In any case, the orientation of the initially formed grains affects the type of diffusion, and hence, the final surface morphology. Orientation of the initially formed grains is not strictly related to the overpotential of the electrodeposition, but to the nucleation processes. However, irregular crystals grown under the conditions of cylindrical diffusion are not found in Pb deposits electrodeposited at overpotentials after the inflection point. The crystals shown in Fig. 3 are not dendrites following the classical definition of a dendrite,¹³ but they behave as dendrites from the electrochemical point of view. This was especially valid for crystals obtained at an overpotential of 75 mV that have sharp tips oriented to the bulk solution. From the electrochemical point of view, a dendrite is defined as an electrode surface protrusion that grows under activation control, while electrodeposition to the macroelectrode is predominantly under diffusion con-

trol.^{15,24,25,27,29,30} Following this definition, the increase of current after the inflection point can be partially ascribed to the activation controlled electrodeposition at the tips of the irregular crystals, and to the strong increase of surface area of the electrode caused by the formation and growth of these forms. In this zone, another two dendritic forms, such as needle-like and fern-like dendrites, are formed with mechanisms of formation somewhat different to those presented in this investigation. The specific mechanism of formation of these types of dendrites will be presented in the future.

It is clear that the irregular crystals shown in Fig. 3 could be considered as microelectrodes situated on the macroelectrodes inside their diffusion layers, as described by Bockris *et al.*^{26,27,31} The majority of current theories concerning the examination of morphology of metal deposits are based on the Barton and Bockris,²⁶ Diggle, Despić and Bockris²⁷ and Despić, Diggle and Bockris³¹ approaches to the examination of metal electrodeposition processes. The Belgrade Electrochemical School also contributed greatly to this field of investigation. This contribution of the Belgrade Electrochemical School to the investigation of the processes of electrochemical deposition, in particular the morphology of electrodeposited metals, was clearly indicated by Bockris.³²

The current theories concerning the electrodeposition of metals are mainly nonspecific dealing with the electrochemical and mass transfer conditions in which some morphological forms of deposits are obtained. This paper is one of the first papers in which specific characteristics of the formation of the determined morphological forms are considered.

CONCLUSIONS

Electrodeposition of lead from 0.40 M $\text{Pb}(\text{NO}_3)_2$ in 2.0 M NaNO_3 at overpotentials belonging to diffusion control was investigated. The technique of scanning electron microscopy (SEM) was used for morphological analysis of the obtained Pb deposits. The morphology of the obtained Pb crystals strongly depended on the orientation of hexagonal-shaped grains formed in the initial stage of electrodeposition. The different shapes formed from the same initial shapes were explained by the effect of orientation of initially formed Pb grains on the type of diffusion. A spherical diffusion layer is formed around the tip of hexagonal-shaped grains oriented with the tip towards the bulk solution. On the contrary, orientation of hexagonal-shaped grains with the lateral side towards the bulk solution causes a cylindrical type of diffusion.

Acknowledgement. The work was supported by the Ministry of Education, Science and Technological Development of the Republic of Serbia under the research project: "Electrochemical synthesis and characterization of nanostructured functional materials for application in new technologies" (No. 172046).

ИЗВОД
УТИЦАЈ ОРИЈЕНТАЦИЈЕ ПОЧЕТНО ФОРМИРАНИХ ЗРНА НА МОРФОЛОГИЈУ
ЕЛЕКТРОХЕМИЈСКИ ИСТАЛОЖЕНОГ ОЛОВА

НЕБОЛША Д. НИКОЛИЋ¹, КОНСТАНТИН И. ПОПОВ^{1,2}, ЕВИЦА Р. ИВАНОВИЋ³ И ГОРАН БРАНКОВИЋ⁴

¹ИХТМ – Центар за електрохемију, Универзитет у Београду, Његишева 12, Београд, ²Технолошко–металуршки факултет, Универзитет у Београду, Карнегијева 4, Београд, ³Пољопривредни факултет, Универзитет у Београду, Немањина 6, Београд–Земун и ⁴Институт за мултидисциплинарна истраживања, Универзитет у Београду, Кнеза Вишеслава 1а, Београд

Процеси електрохемијског таложења олова у условима дифузионе контроле су испитивани анализом добијених кристала техником скенирајуће електронске микроскопије. Оријентација зрна хексагоналног облика формираних у почетној фази електрохемијског таложења је снажно утицала на крајњу морфологију кристала олова. Формирање кристала олова различитог облика од истог почетног облика је дискутовано преко утицаја оријентације почетно формираних зрна на тип дифузионе контроле. Сферични дифузиони слој формира се око врха зрна хексагоналног облика оријентисаног врхом ка дубини раствора, доводећи до формирања издужених кристала током процеса раста. На другој страни, цилиндрични тип дифузије је одговоран за раст хексагонално обликованих зрна оријентисаних бочном страном ка дубини раствора. Кристали олова са добро дефинисаним странама паралелним површини макроелектроде се формирају овим типом дифузије.

(Примљено 11. децембра 2013, ревидирано 20. јануара, прихваћено 21. јануара 2014)

REFERENCES

1. C.-Z. Yao, M. Liu, P. Zhang, X.-H. He, G.-R. Li, W.-X. Zhao, P. Liu, Y.-X. Tong, *Electrochim. Acta* **54** (2008) 247
2. D. Pavlov, *J. Power Sources* **42** (1993) 345
3. B. Rashkova, B. Guel, R. T. Potzschke, G. Staikov, W. J. Lorenz, *Electrochim. Acta* **43** (1998) 3021
4. C. Ehlers, U. Konig, G. Staikov, J. W. Schultze, *Electrochim. Acta* **47** (2002) 379
5. C. O. Avellaneda, M. A. Napolitano, E. K. Kaibara, L. O. S. Bulhoes, *Electrochim. Acta* **50** (2005) 1317
6. R. Winand, *Electrochim. Acta* **39** (1994) 1091
7. V. M. Kozlov, L. Peraldo Bicelli, *J. Cryst. Growth* **203** (1999) 255
8. N. D. Nikolić, K. I. Popov, P. M. Živković, G. Branković, *J. Electroanal. Chem.* **691** (2013) 66
9. N. D. Nikolić, Dj. Dj. Vaštag, P. M. Živković, B. Jokić, G. Branković, *Adv. Powder Technol.* **24** (2013) 674
10. N. D. Nikolić, Dj. Dj. Vaštag, V. M. Maksimović, G. Branković, *Trans. Nonferrous Met. Soc. China* **24** (2014) 884
11. N. D. Nikolić, G. Branković, U. Lačnjevac, *J. Solid State Electrochem.* **16** (2012) 2121
12. N. D. Nikolić, V. M. Maksimović, G. Branković, *RSC Adv.* **3** (2013) 7466
13. G. Wranglen, *Electrochim. Acta* **2** (1960) 130
14. N. D. Nikolić, V. M. Maksimović, G. Branković, P. M. Živković, M. G. Pavlović, *J. Serb. Chem. Soc.* **78** (2013) 1387
15. K. I. Popov, S. S. Djokić, B. N. Grgur, *Fundamental aspects of electrometallurgy*, Kluwer Academic/Plenum Publishers, New York, 2002, p.p. 1–305
16. I. Markov, A. Boynov, S. Toshev, *Electrochim. Acta* **18** (1973) 377

17. K. I. Popov, B. N. Grgur, E. R. Stojilković, M. G. Pavlović, N. D. Nikolić, *J. Serb. Chem. Soc.* **62** (1997) 433
18. N. Ya. Kovarskii, A. V. Lisov, *Elektrokhimiya* **20** (1984) 221 (in Russian)
19. N. Ya. Kovarskii, A. V. Lisov, *Elektrokhimiya* **20** (1984) 833 (in Russian)
20. N. Ya. Kovarskii, A. V. Lisov, *Elektrokhimiya* **20** (1984) 452 (in Russian)
21. K. I. Popov, P. M. Živković, N. D. Nikolić, *J. Serb. Chem. Soc.* **76** (2011) 805
22. K. I. Popov, M. I. Čekerevac, *Surf. Technol.* **37** (1989) 435
23. I. M. Epstein, *Elektrokhimiya* **2** (1966) 734 (in Russian)
24. K. I. Popov, N. V. Krstajić, M. I. Čekerevac, in *Modern Aspects of Electrochemistry*, R. E. White, B. E. Conway, J. O'M. Bockris, Eds., Vol. 30, Plenum Press, New York, 1996, p.p. 261–312
25. K. I. Popov, N. D. Nikolić, in *Modern Aspects of Electrochemistry*, S. S. Djokić, Ed., Vol. 54, Springer, Berlin, 2012, p.p. 1–62
26. J. L. Barton, J. O'M. Bockris, *Proc. Roy. Soc., A* **268** (1962) 485
27. J. W. Diggle, A. R. Despić, J. O'M. Bockris, *J. Electrochem. Soc.* **116** (1969) 1503
28. J. S. Newman, *Electrochemical Systems*, Prentice-Hall, Inc. Engelwood Cliffs, NJ, 1973
29. A. R. Despić, K. I. Popov, in *Modern Aspects of Electrochemistry*, B. E. Conway, J. O'M. Bockris, Eds., Vol. 7, Plenum Press, New York, 1972, p.p. 199–313
30. K. I. Popov, P. M. Živković, N. D. Nikolić, in *Modern Aspects of Electrochemistry*, S. S. Djokić, Ed., Vol. 48, Springer, New York, 2010, p.p. 163–213
31. A. R. Despić, J. W. Diggle, J. O'M. Bockris, *J. Electrochem. Soc.* **116** (1969) 507
32. J. O'M. Bockris, A. K. N. Reddy, *Modern Electrochemistry 1, Ionics*, Plenum Press, New York and London, 1998, p. 2.